

1 **Kinetic modeling and parameter estimation of a prebiotic peptide reaction network**2 **Authors**3 *Hayley Boigenzahn^{1,2}, Leonardo D. González¹, Jaron C. Thompson¹, Victor M. Zavala¹, John*
4 *Yin^{1,2*}*

5 *Corresponding Author: john.yin@wisc.edu

6 **Affiliations**7 ¹Department of Chemical and Biological Engineering, University of Wisconsin-Madison, 1415
8 Engineering Drive, Madison, WI 53706, USA9 ²Wisconsin Institute for Discovery, University of Wisconsin-Madison, 330 N. Orchard Street,
10 Madison, WI 53715, USA

11

12

13 **Abstract**14 Although our understanding of how life emerged on Earth from simple organic precursors is
15 speculative, early precursors likely included amino acids. The polymerization of amino acids into
16 peptides and interactions between peptides are of interest because peptides and proteins
17 participate in complex interaction networks in extant biology. However, peptide reaction
18 networks can be challenging to study because of the potential for multiple species and systems-
19 level interactions between species. We developed and employed a computational network model
20 to describe reactions between amino acids to form di-, tri-, and tetra-peptides. Our experiments
21 were initiated with two of the simplest amino acids, glycine and alanine, mediated by
22 trimetaphosphate-activation and drying to promote peptide bond formation. The parameter
23 estimates for bond formation and hydrolysis reactions in the system were found to be poorly
24 constrained due to a network property known as sloppiness. In a sloppy model, the behavior
25 mostly depends on only a subset of parameter combinations, but there is no straightforward way
26 to determine which parameters should be included or excluded. Despite our inability to
27 determine the exact values of specific kinetic parameters, we could make reasonably accurate
28 predictions of model behavior. In short, our modeling has highlighted challenges and
29 opportunities toward understanding the behaviors of complex prebiotic chemical experiments.

30

31 **Keywords**

32 Peptides, chemical reaction networks, kinetics, parameter estimation, prebiotic chemistry

33 **Introduction**

34 The emergence of life on the early Earth is believed to have been preceded by the
35 accumulation of an increasingly diverse and complex set of organic molecules (Orgel 2010). The
36 reaction networks developed by these molecules laid the groundwork of functions critical for
37 life, like energy and information processing. Understanding how the systems-level molecular
38 interactions required for life-like behavior could emerge from simple precursors remains one of
39 the key questions of prebiotic chemistry, but since this question is primarily about collective
40 behaviors, complexity presents an ongoing challenge (Schwartz 2007; Johnson & Hung 2019).
41 While studying a single type of molecule or a single reaction to establish its properties can be
42 useful, it limits what conclusions can be drawn about potential broader community behavior.
43 Experiments involving a greater variety of molecules and reactions can probe more interesting
44 interactions, but have a large search space of variables, and the complexity of the systems make
45 them inherently more difficult to analyze.

46 Models are useful for understanding complex systems because they can reveal the systematic
47 dependence of various properties on each other and allow us to describe and make predictions
48 about the system behavior. Computational models have been used to explore hypothetical
49 prebiotic chemical networks for many years and have produced many interesting insights
50 (Covney et al. 2012). However, our current interest is in models that are based on experimental
51 data. Prior experimental works mainly used basic kinetic and thermodynamic governing
52 equations to describe individual reactions or small networks involving fewer than five reactions.
53 For example, Arrhenius expressions have been used to determine the free energies of activation
54 for reactions in a small network (Sakata et al. 2010; Yu et al. 2016; Lee et al. 1996). More
55 abstractly, parameters have been fit to empirical rate equations to describe specific elements of
56 system behavior or distinguish between candidate models (von Kiedrowski 1986; Rout et al.
57 2022). These methods work well for small systems, but may not apply to larger systems with
58 multiple reactions occurring simultaneously and potentially more intricate network interactions.
59 Serov et al. (2020) approximated the parameters for multiple reactions simultaneously in a
60 peptide reaction network, but the parameter fitting was performed manually, and the network
61 was small. Manual approaches are less rigorous than using a computational strategy and can be
62 difficult to implement for even moderately sized networks. On the other hand, results from more
63 complex experiments have been analyzed using statistical methods, but these do not capture the
64 system dynamics (Surman et al. 2019; Jain et al. 2022). There is a need for approaches to study
65 the dynamical behavior of more complex experimental networks (Ruiz-Mirazo et al. 2014).

66 Complex network models are broadly applicable and have already been developed
67 extensively for other fields (Newman 2003). One notable example is in systems biology, which
68 has significant parallels to the origins of life. Both involve large interaction networks with
69 potentially limited available data and may include community interactions that are critical to
70 understanding system behavior. Bioinformatics models can be used to analyze experimental data
71 and help understand the molecular interaction networks within living cells (Gauthier et al. 2019).

72 Similar approaches could be useful for furthering experimental chemical origins of life research,
73 but aside from a few reviews and computational investigations, they have generally been
74 overlooked (Johnson & Hung 2019; Ludlow & Otto 2008; Goldman et al. 2013).

75 Our goal in this study was to investigate how dynamical models, described by ordinary
76 differential equations (ODEs), might be useful for studying origins of life chemistry. These
77 models are theoretically generalizable, but as with all modeling approaches, there are limitations
78 that make them more difficult to apply in some situations. Presenting the benefits and limitations
79 of a model approach in a way that is accessible to experimentalists, which we aim to do, is an
80 important step for linking theory and experiment. Differential equation models are not always
81 suitable for large systems, since constructing them can become difficult, but in well-defined
82 systems they can be used to study detailed mechanistic behavior (Maria 2004). Computational
83 methods can be used to estimate all the parameters efficiently and simultaneously in a
84 moderately complex dynamical network, but validating the physical meaning of the results can
85 be more challenging since these problems may not have a unique and stable solution (Transtrum
86 et al. 2015). However, parameter fitting has still been used to describe nonlinear networks in a
87 variety of fields, including in systems biology for biochemical pathways (Raue et al. 2013;
88 Rodriguez-Fernandez et al. 2006).

89 We focus specifically on fitting parameters to a set of nonlinear ODEs describing the kinetics
90 of short peptide formation. Peptides are interesting candidates for emergent behavior because
91 they can engage in a variety of intermolecular interactions and their development was likely an
92 important step during the origin of life (Frenkel-Pinter et al. 2020). We studied a simplified
93 network describing peptide formation in a system starting with only two amino acid species,
94 glycine and alanine. By limiting ourselves to two amino acids, we were able to obtain
95 quantitative data on the concentrations of most peptide species as they formed through a possible
96 prebiotic reaction mechanism involving an inorganic phosphate activating agent,
97 trimetaphosphate (TP) (Sibilska et al. 2018).

98 We found that our model exhibited “sloppiness”, a term originally used by the Sethna lab
99 to describe models based on a set of highly imprecise parameters that still return reasonably
100 accurate predictions (Gutenkunst et al. 2007a). Such models are significantly more sensitive to
101 changes in certain parameter values while remaining largely unaffected by changes in others
102 (Waterfall et al. 2006). We suspect sloppiness may be a common feature in networks relevant to
103 the chemical origin of life. It is known to be extremely common in systems biology, and many of
104 the features that contribute to it, like reversibility of reactions and limited experimental
105 observations, are also common features of prebiotic chemistry networks (White et al. 2016).

106 Sloppiness occurs when parts of the parameter fitting problem are poorly constrained,
107 resulting in highly imprecise parameter estimates. Our computational study reveals that the
108 peptide network model is sloppy. Due to their high uncertainty, parameters fitted to a sloppy
109 model cannot be treated as true kinetic reaction rates, limiting the hypotheses a sloppy model can

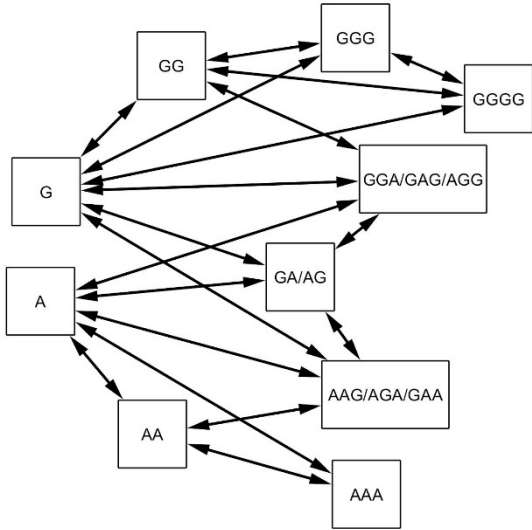
110 be used to evaluate (Gutenkunst et al. 2007a). However, the collective behavior predicted by
111 fitting a sloppy model can be accurate even when fit to relatively sparse experimental data. This
112 makes them useful for tasks such as exploring theoretical long-term behavior and model
113 falsification (Brown et al. 2004; Gutenkunst et al. 2007b; Hettling & van Beek 2011). For these
114 reasons, we concluded that this system was worth investigating and disseminating despite the
115 high variability observed in the parameter estimates.

116 We attempted to reduce sloppiness using model reduction and statistical design of
117 experiments, but without improvements. As such, it is important to recognize the inherent
118 limitations of the model structure and of the experimental setup. We conclude that fitting
119 accurate kinetic parameters using the approach we present might be difficult. However, ODE
120 models can still be useful tools for characterizing the behavior and stability of prebiotic chemical
121 reaction networks.

122 *Methods*

123 We studied the formation of peptides from amino acids using trimetaphosphate (TP) as an
124 activating agent. For simplicity, our experiments only included two amino acids: glycine and
125 alanine. To maximize peptide bond formation within 24 hours, samples at alkaline pH were
126 allowed to dry completely (Sibilska et al. 2018). Various combinations of initial concentrations
127 of glycine and alanine were used to increase the amount of relevant data for parameter fitting,
128 and cover a larger range of potential conditions in the network, since concentrations of each
129 species should not affect the values of the kinetic constants. The concentrations of each peptide
130 product were determined using HPLC (see Experimental Methods for details). Each
131 experimental data point is the average of three experimental replicates.

132 Parameters were fit to an ODE model describing peptide formation and decomposition in
133 a mass-action style network, depicted in Fig. 1. The complete time-dependent ODEs for the
134 model are provided in Supplementary Information 1. To keep the network a manageable size, we
135 omitted many mechanistic details of peptide formation and only includes canonical peptides, not
136 intermediates or possible side products. For example, no phosphate salts or intermediate products
137 of TP activation were quantifiable in our analysis, so TP was not explicitly included anywhere in
138 the network. To minimize any effect the concentration of TP might have on the kinetics studied,
139 we used a constant ratio of TP to amino acids across all experiments. Isomers such as GGA,
140 GAG, and AGG were grouped together to further reduce the number of parameters and avoid the
141 need to resolve isomers, which tend to co-elute during HPLC analysis. A complete list of fitted
142 parameters, organized by figure, are available on Github at
143 <https://github.com/haboigenzahn/OoL-KineticParameterEstimation>.



144

145 **Figure 1: Peptide network.** Double-headed arrows represent a reversible reaction connecting
 146 two species. Note that many edges share the same reaction parameter, such as the $G \rightarrow GGG$ and
 147 $GG \rightarrow GGG$ edges representing the reaction $G+GG \rightarrow GGG$.

148 We expected that the network would provide a good baseline for understanding which
 149 reactions were occurring at higher rates. To improve the precision of the parameter estimates, we
 150 applied model reduction and statistical experimental design. Details about these approaches can
 151 be found in the Computational Methods section. Here we will describe the results of these tests
 152 and assess the feasibility of obtaining a predictive model and accurate parameter estimates from
 153 experimental data.

154 *Results & Discussion*

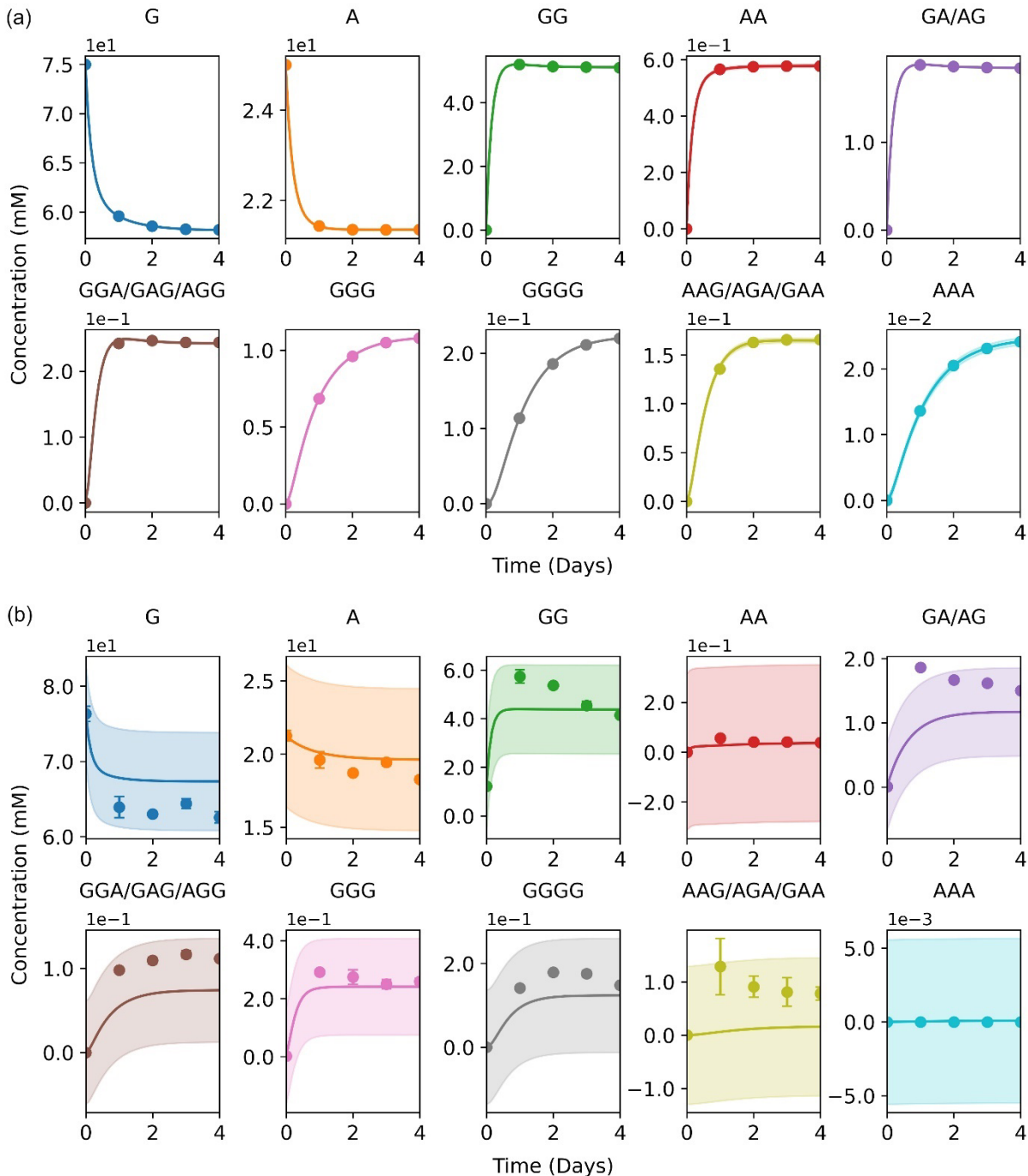
155 *Parameter Estimation*

156 Parameter fitting is performed by tuning the model parameters to minimize a *cost*
 157 *function* (\mathcal{L}) that calculates the difference between the model predictions and experimental data;
 158 \mathcal{L} is also called a loss function or a residual. We minimized \mathcal{L} using the L-BFGS-B algorithm
 159 from Scipy's minimize function (Virtanen et al. 2020). We were also able to approximate the
 160 parameter uncertainties, which represent how well the parameters are constrained by
 161 experimental data using an asymptotic Gaussian approximation (Vanlier et al. 2013). Parameters
 162 determined using sparse or noisy experimental data are less precise than parameters fit with
 163 abundant, high precision data, but the structure of the model itself can also significantly
 164 contribute to the parameter uncertainty. Validating that the model can theoretically be solved can
 165 save time and experimental effort.

166 We first estimated the parameters for simulated data in the absence of noise, and we were
 167 able to accurately recover the parameters used to generate the data (Fig. 2a). When we applied
 168 the model to experimental data, it was able to capture general trends. However, the parameter
 169 uncertainties were undesirably high (Fig. 2b). For some species, the 95% confidence envelope

170 for the model prediction was larger than the peptide concentrations themselves. Since the
171 optimization can find a local minimum, we repeated the parameter estimation for several
172 different initial guesses. Although the number of initial guesses was limited by the fact that the
173 parameter estimation method can take a full day to finish when all of the experimental data is
174 included, we observed that none of the different initial guesses significantly improved the
175 precision of the parameter estimates and that there did not appear to be any positive correlation
176 between the MSE and the number of highly uncertain parameters (Supplementary Information
177 2). Trying many initial guesses to find the lowest possible value for the cost function may
178 slightly improve the model predictions, but it does not seem to cause an improvement in the
179 precision of the parameter estimates. Despite the extremely high parameter uncertainties, the
180 accuracy of the model predictions initially seemed promising, so we began to explore the
181 parameter fitting process in more detail to determine how to decrease the parameter uncertainty,
182 starting with the identifiability of the network.

183



184 **Figure 2: Comparison of fitting data and model predictions.** Results are shown for (a)
185 simulated data and (b) experimental data, using initial conditions of 75 mM glycine and 25 mM
186 alanine. Both the simulated and experimental data sets included 65 data points and the simulated
187 data had no artificially added noise.

188

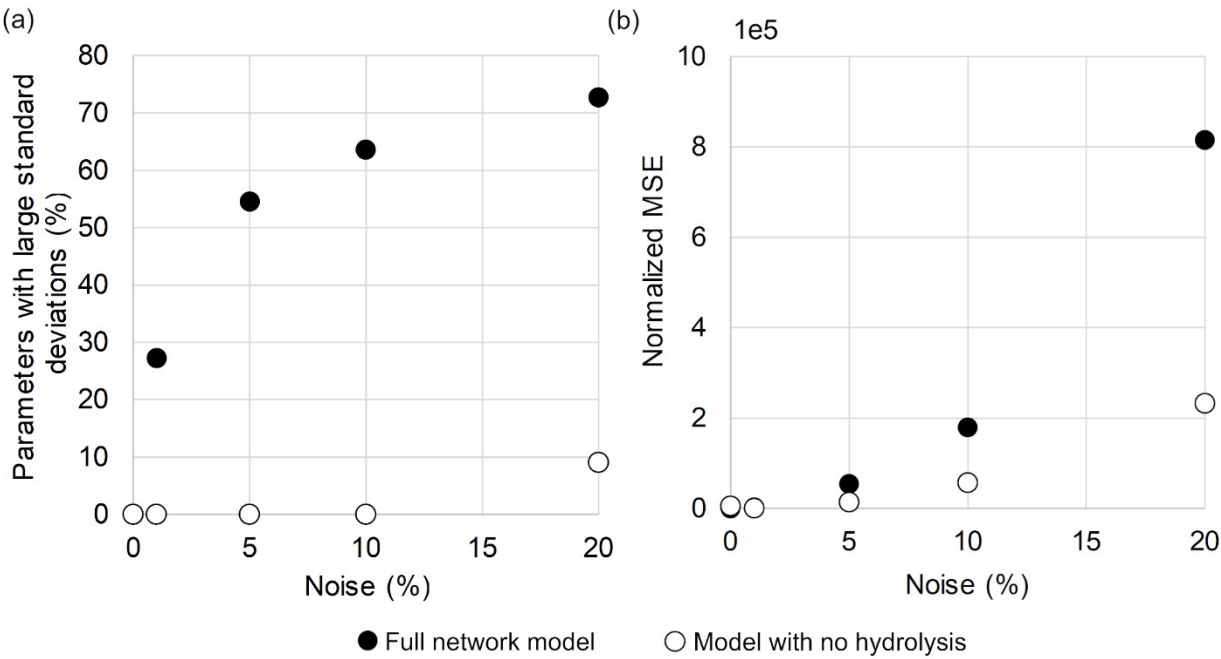
189 *Identifiability & Sloppiness*

190 Identifiability analysis determines the possibility of a unique and precise estimate of the
191 unknown parameters in a network (Cobelli & DiStefano, 1980; Wieland et al. 2021). If a unique
192 solution cannot be obtained, then the model is said to be *structurally unidentifiable*. A model is
193 *practically unidentifiable* if its parameters cannot be estimated at an acceptable level of
194 precision. The exact definition of what is considered an acceptable level of precision varies from
195 case to case. Practical unidentifiability indicates that regions of the objective function are
196 relatively flat, making it difficult to find a minimum and it typically results from overfitting
197 (White et al. 2016). Finally, some models exhibit a property known as *sloppiness*, which occurs
198 when its behavior is highly sensitive to changes in certain combinations of parameters and
199 almost completely insensitive to changes in others (Gutenkunst et al. 2007a). Generally,
200 sloppiness is a consequence of the model structure and its input range (White et al. 2016).
201 Although sloppiness and practical unidentifiability are not synonymous, in practice they often
202 coincide (Chis et al. 2014).

203 Sloppiness can be recognized by examining the spectrum eigenvalues of the Hessian
204 matrix, sometimes called the sensitivity eigenvalues (see Computational Methods section for
205 further detail) (Gutenkunst et al. 2007a). The sensitivity eigenvalues are an indirect estimate of
206 the sensitivity of the cost function to changes in the parameter values and represents the
207 confidence in the estimate of the parameter combination in the direction of the corresponding
208 eigenvector. Small eigenvalues represent high uncertainties and large confidence intervals.
209 Sloppy models have sensitivity eigenvalues that are roughly evenly spaced across three or more
210 orders of magnitude. When the eigenvalue spectrum is this large, the smallest sensitivity
211 eigenvalues tend to correspond to parameter combinations that have minimal effect on the model
212 behavior – these combinations are ‘sloppy’ eigenvectors. The eigenvectors of the largest
213 eigenvalues are referred to as ‘stiff’ and control most of the model behavior. In some models,
214 there is a clear division between the large and small eigenvalues, usually corresponding to a clear
215 separation in length or time scales that renders some of the physical details of the system
216 irrelevant – for example, the kinetic models of many chemical reactions can be simplified when
217 there is a known rate-limiting step (White et al. 2016). In sloppy models, no clear division exists,
218 and the small eigenvalues are rarely united by a single physical phenomenon.

219 Since rigorously checking for structural identifiability in nonlinear models can be
220 challenging, we tested the identifiability of our model by determining if it could recover the
221 parameters used to generate a set of noiseless, simulated data. We found that all parameters could
222 be recovered with acceptably high accuracy, suggesting that the model was identifiable. Here, we
223 define acceptable accuracy to be when a parameter’s standard deviation is at least one order of
224 magnitude smaller than value of the associated parameter. However, when we examined the
225 effect of noise on model performance, we observed that the parameter standard deviations rise
226 rapidly when even a small amount of noise is introduced (Fig. 3a). The error of the model
227 predictions, on the other hand, rose relatively slowly as noise increased. This suggests that

228 despite the high parameter uncertainties, the general behavior predicted by the model can be
 229 accurate even when it is fit using noisy data (Fig. 3b).

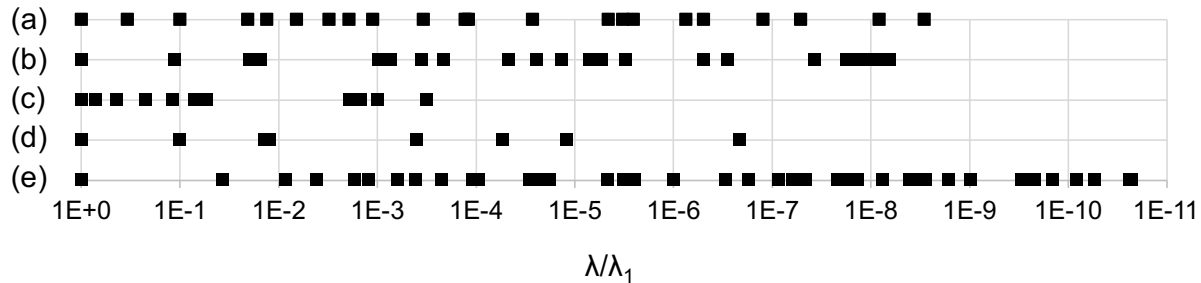


230 **Figure 3: Comparison of parameter accuracy and mean squared error (MSE) for two**
 231 **different network structures at various noise levels.** For the full reaction network, as the noise
 232 in the input data is increased, (a) the number of parameters with standard deviations within one
 233 order of magnitude of the parameter value rises rapidly compared to (b) the error of the model
 234 predictions. When the hydrolysis reactions are removed from the full network, the parameter
 235 estimates remain relatively precise as noise is introduced. The MSE of the model predictions are
 236 normalized to the MSE of the full network with no artificial noise (2.85e-11). All data sets used
 237 simulated experiments created from 25 different initial conditions and 125 data points. The
 238 added noise was normally distributed with a constant signal-to-noise ratio, and all negative
 239 values were set to zero to prevent negative concentrations.

240 Given that this behavior is typical in sloppy models, we checked the sensitivity
 241 eigenvalues for both our simulated data and experimental data (Fig. 4a, b). We found that the
 242 peptide reaction network is unambiguously sloppy, because the sensitivity eigenvalues of the
 243 simulated and experimental data span nearly nine and seven orders of magnitude respectively. To
 244 compare the behavior of the peptide reaction network with a similar model that was not sloppy,
 245 we modified the network to exclude all hydrolysis reactions (Supplementary Information 3a).
 246 Removing reversible pathways from the network eliminates many combinations of parameters
 247 that can compensate for one another, which significantly reduced sloppiness (Fig. 4c). To
 248 demonstrate that it was the modifications to the structure of the model, rather than its smaller
 249 size, that were responsible for the reduction in sloppiness, we also compared it to an even smaller
 250 network describing reversible homopolymer reactions (Supplementary Information 3b); this

251 model was determined to have a much larger eigenvalue span (Fig. 4d). To investigate whether
 252 the grouping of some species in the peptide network was responsible for the sloppiness of the
 253 model, we also checked the sensitivity eigenvalues for a network with the trimer species
 254 separated using simulated data (Supplementary Information 3c), and found it made the
 255 eigenvalue spread larger (Fig. 4e).

256 The parameter standard deviations were far more sensitive to noise in the full, sloppy
 257 network than in the network with no hydrolysis reactions (Fig. 3a). Despite the difference in the
 258 confidence of the parameter fits, the prediction accuracy was not significantly different between
 259 the two models until significant noise was added to the data (Fig. 3b). This demonstrates a
 260 previously mentioned key consequence of sloppy models – although they can make reasonably
 261 accurate predictions of system behavior, they should not be used to calculate the values of
 262 individual parameters, since the precision required for accurate parameter estimations cannot be
 263 experimentally realized.



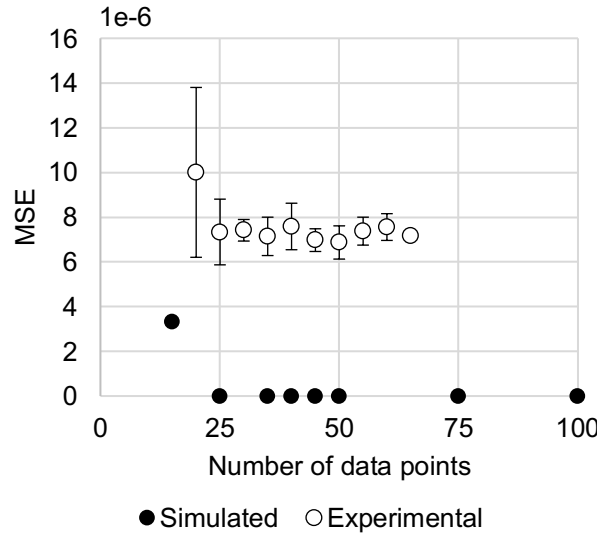
264 **Figure 4: Sensitivity eigenvalues for different models:** (a) simulated data for the full network
 265 (22 parameters, 35 data points), (b) experimental data generated from a mixture of glycine and
 266 alanine (22 parameters, 65 data points), (c) simulated data for a variation of the main network
 267 that excludes all hydrolysis reactions (11 parameters, 35 data points), (d) simulated data for
 268 network including only one amino acid forming peptides up to tetramer length with hydrolysis
 269 reactions included (8 parameters, 35 data points) and (e) simulated data for a network with
 270 separated trimers (40 parameters, 80 data points). Each system is normalized to its largest
 271 eigenvalue (λ_1). All simulated data has no additional noise included.

272 Sloppiness is a common property in systems biology models, and some of the
 273 characteristics that result in sloppiness are likely shared by prebiotic chemistry systems.
 274 Reversible reactions and cyclic behaviors can increase the likelihood of sloppiness because they
 275 create situations where a particular combination of parameters (for example, the ratio between
 276 forward and reverse rates defining an equilibrium constant) is more important for describing the
 277 system behavior than the individual parameters themselves. The parameters may become
 278 ‘sloppy’ because their individual values can essentially vary freely without affecting the overall
 279 model behavior, as long changes in other parameters can compensate to produce a similar overall
 280 prediction. Reaction networks that are mostly or entirely reversible, like the peptide reaction
 281 network, can therefore become significantly more difficult to fit with high precision than models

283 with comparable sizes, but fewer reversible reactions (Maity et al. 2020). The emergence of
284 cycles and reversible reactions are expected to be important features in the emergence of life-like
285 chemistry (Varfolomeev & Lushchekina 2014; Mamajanov et al. 2014). Therefore, we anticipate
286 that sloppiness may be a common and potentially unavoidable feature of ODE models found in
287 prebiotic chemistry, and its implications should be examined.

288 *Consequences of Collective Fitting*

289 Sloppy models can provide surprisingly accurate predictions despite having low
290 confidence parameter estimates. The collective fit of all the parameters tends to be more accurate
291 and require less data than the individual parameter uncertainties might suggest, since only the
292 stiff parameter combinations must be constrained to achieve accurate predictions. One of the
293 consequences of collective fitting is that the numerical values of parameters estimated for sloppy
294 models cannot be treated as independent kinetic parameters whose quantitative values have
295 physical meaning. Situations where a reaction occurs faster in the presence of one molecule than
296 another are of interest to the chemical origins of life because of their semblance to catalysis.
297 Unfortunately, in sloppy models, the numerical values of the parameters fit in each case are often
298 not comparable. For example, even if the rate constant of one reaction in the peptide network
299 was significantly higher than another, that is not necessarily good evidence that one reaction
300 proceeds faster than the other. The parameters are only meaningful when the entire system is
301 used to describe the specific environment to which they were fit. Fixing individual parameter
302 values to reflect direct measurements or literature values can potentially break the collective fit
303 and significantly increase the error of the prediction, often to the point that it is no longer useful.
304 The lack of physical meaning of the individual parameter values is a significant drawback of
305 sloppy models. However, such models can still be useful for certain tasks. For example, a sloppy
306 model can still be used if the goal is to generate predictions about the behavior of a similar
307 system with slightly different initial conditions, or to predict responses at longer time spans.
308 Moreover, we highlight that sloppiness might simply be a fundamental property of the actual
309 reaction network, that arises from inherent redundancies in the system.



310

311 **Figure 5: MSE of model predictions depend on quantity of experimental and simulated**
 312 **data.** Except for the final points, which include all applicable data, parameters were estimated
 313 for three arbitrarily selected data subsets of varying sizes, then the average MSE of those models
 314 was determined. Noise was neglected. Error bars show the standard deviation of the three
 315 subsets, but are too small to be visible for the simulated data.

316 To estimate the minimal data required to get relatively accurate predictions, we created at
 317 least three different subsets of the data, trained the model individually with each subset, and
 318 compared their MSEs (Fig. 5). The simulated data was sampled at time intervals analogous to the
 319 experimental results, since those were the points that were physically relevant. When training the
 320 model using simulated data, increasing the amount of data used improved the model predictions
 321 up to about 40 data points, but with even 25 data points, the error was negligible compared to the
 322 experimental results. Similarly, when we repeated the process with experimental data, the
 323 average error did not decrease as more data was added beyond 25 data points.

324 We also investigated the effect of using more frequent measurements, as opposed to using
 325 a greater number of simulated experiments with different initial conditions. We compared the
 326 results of simulated data with a similar number of total data points, but double the usual
 327 sampling frequency to the simulated results in Fig. 5. Increasing the sampling frequency was
 328 comparable or slightly worse than including data from additional simulated initial conditions,
 329 except possibly when there is little data available overall (Supplementary Information 4). It did
 330 not improve the model's sensitivity to noise.

331 Different subsets of the data with the same number of data points could have fairly
 332 different MSEs, suggesting that some combinations of experiments may be better for parameter
 333 fitting than others. This subject will be discussed further in the section on the design of
 334 experiments (DoE). Overall, these results suggest that as few as 25 to 30 data points are required
 335 to fit the system as accurately as the model constraints allow; therefore reasonably accurate

336 predictive fits can be achieved with a realistically obtainable amount of data. The ability to
337 extrapolate accurate model predictions from short-term experiments has some uses for studying
338 prebiotic chemical reactions, since long time spans are potentially relevant. Models like the one
339 we present here could be used to predict the expected equilibrium outcome of slow reactions
340 based on data from a shorter time span and compare candidate model structures. They may also
341 be a useful way to predict the outcomes of sequential or cyclic processes, provided that the
342 parameters are fit in compatible experimental conditions. Sensitivity analysis can be used to
343 validate the predictions from sloppy models independently from the parameter uncertainties
344 (Gutenkunst et al. 2007a). Model selection, which involves comparing two or more different
345 model structures to determine which one reflects the experimental data most accurately, can also
346 still be performed with sloppy models (Brown & Sethna 2003). However, if finding physically
347 meaningful terms for the parameter values is an important goal, then the aim should be to reduce
348 the sloppiness of the model.

349 *Model Reduction*

350 To address high parameter uncertainty, one may seek to simplify the structure of the
351 model, ideally without compromising the accuracy of the model predictions. This task is referred
352 to as *model reduction* or *network reduction*, and it can be an effective way to improve
353 overparameterized models (Apri et al. 2012; Transtrum et al. 2015). However, model reduction
354 methods are generally based on statistical principles and not physical knowledge, and the results
355 should be interpreted within an experimental context. The user must ensure that parameters that
356 might be statistically problematic but are known to be physically significant are not removed
357 from the model.

358 Since one of the main features of sloppy models is that they contain parameter
359 combinations that are insensitive to changes, model reduction may initially appear to be a
360 straightforward task for sloppy models. However, the fact that the sensitivity eigenvalues are
361 evenly distributed over multiple orders of magnitude poses a challenge for accurate model
362 reduction, as there is no clear cut-off between the parameter combinations that are important and
363 those that are not. Additionally, in practice some parameters are so poorly constrained that they
364 are randomly distributed throughout the sensitivity eigenvectors, so the components of the
365 sensitivity eigenvectors are not entirely reliable indicators of what parameters are influencing
366 them (Gutenkunst et al. 2007a).

367 We attempted model reduction with the peptide reaction network to determine if it was
368 over-parameterized and if it might be possible to reduce the reactions considered. For example,
369 we expected that some of the hydrolysis reactions could be ignored. Since we wanted to use a
370 model reduction technique that is accessible and easily interpretable for experimentalists, we
371 used sparse principal component analysis (SPCA). SPCA is an extension of principal component
372 analysis (PCA), a popular dimensionality reduction method for linear models (Zou et al. 2006).
373 Using SPCA, we can identify the inputs that capture most of the information in the data. It has

374 been used successfully in control theory and gene network analysis, and there are existing
375 implementations of it in MATLAB and Python (Ma & Dai 2011).

376 When SPCA was applied to the peptide reaction network, the results were highly variable
377 and unable to adequately represent the data. SPCA frequently suggested removing reactions
378 known to be physically significant, such as the formation of dimers from monomers
379 (Supplementary Information 5). Not only does this not make physical sense, but because these
380 are the initial reactions that occur in the system, removing them severely limits the pathways for
381 longer species to form. Other methods of network reduction may be more effective for sloppy
382 models, but are less commonly used and may be more difficult to implement (Transtrum & Qiu
383 2014; Maiwald et al. 2016). If we choose to pursue additional model reduction efforts, one
384 logical next step may be to inspect the inverse of the covariance matrix to identify which
385 parameters are the most correlated and least constrained by the data (Wasserman, L. 2004). This
386 information may be useful for determining which parameters are best to remove or to combine
387 into a single term.

388

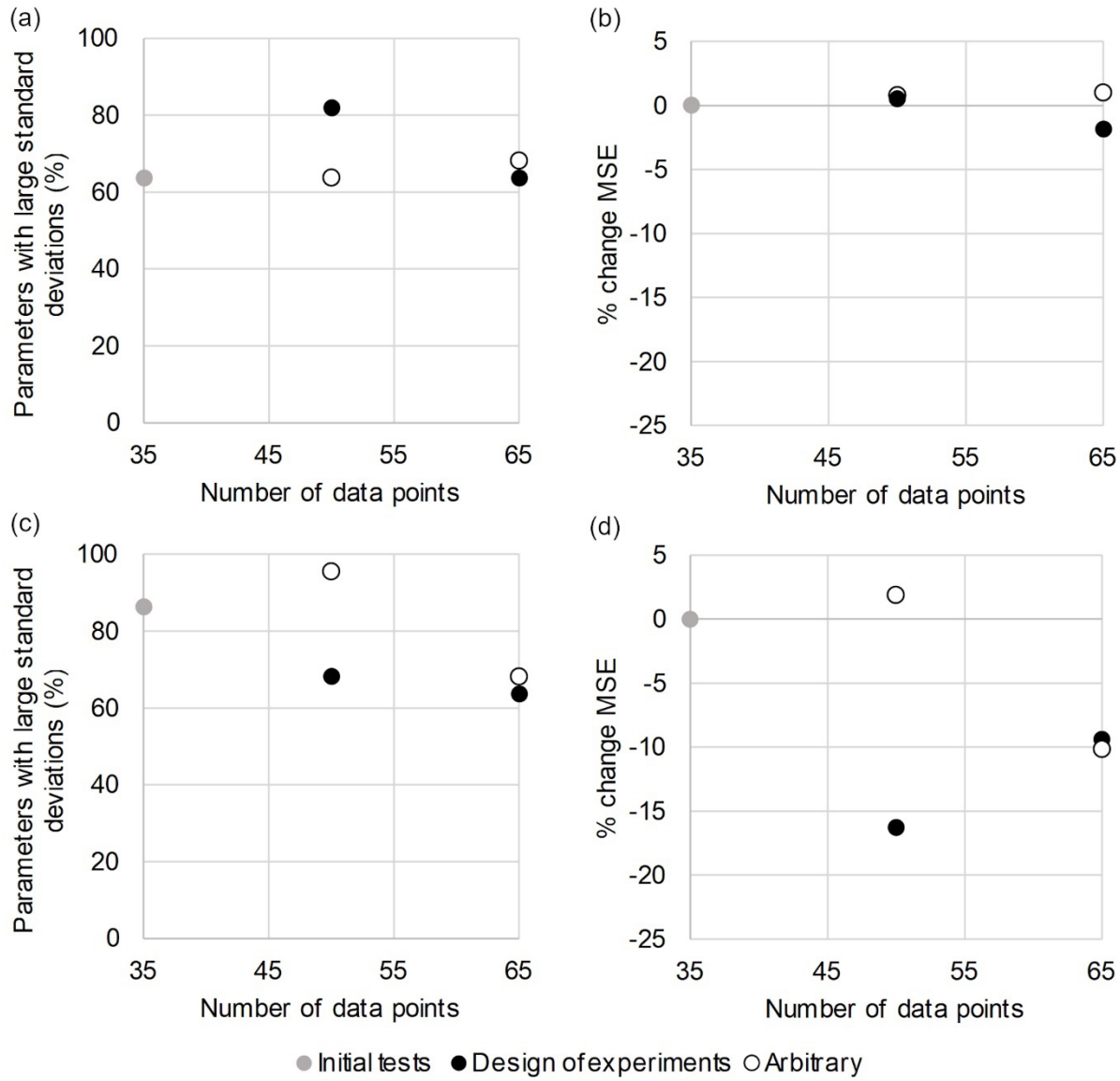
389 *Design of Experiments*

390

391 If the model structure cannot be altered, another method for reducing sloppiness is to
392 determine if experimental data can be gathered strategically to explore the variable space more
393 thoroughly (Apgar et al. 2010). However, to reduce parameter uncertainty, the selected
394 experiments must provide new information not already captured in the model. *Design of*
395 *experiments* (DoE), or experimental design, seeks to identify the experiments that would provide
396 the most useful information for improving prediction accuracies. DoE methods such as factorial
397 design (Fisher 1935), response surface methodology (Box & Wilson 1951), and screening
398 (Shevlin 2017), have been widely adopted across various fields. However, there are several
399 notable caveats in relation to sloppy models (Jagadeesan et al. 2022). First, the precision of
400 parameter fitting for sloppy models is limited by the least accurately determined eigenvectors, so
401 more data measured with the same uncertainty may not help. Second, there is some debate over
402 whether DoE can be used with approximate models without risking the collective fit, as it can
403 inadvertently place too much importance on details not included in the model (White et al.
404 2016).

405 In this work, we use a Bayesian experimental design (BED) method that selects
406 experimental designs based on the expected reduction in parameter uncertainty as quantified by
407 the determinant of the Fisher information matrix (FIM) (Transtrum et al. 2012; Thompson et al.
408 2022). To determine if there was any significant benefit obtained using DoE, we compared the
409 reduction in parameter uncertainty from performing experiments suggested by the BED method
410 to the reduction achieved from performing arbitrarily chosen experiments (Fig. 6). We evaluated
411 the results using a couple of matrices – the percentage of parameters with standard deviations
412 that were large (within an order of magnitude of the relevant parameter) to indicate the overall

413 precision of the parameter estimates, and by the MSE to indicate the accuracy of the model's
 414 predictions.



415

416 **Figure 6: DoE slightly improved the precision of the parameter estimates and the model**
 417 **prediction accuracy.** (a) Using simulated data with 15% noise, the percentage of large
 418 parameter uncertainties (standard deviation within one order of magnitude of the parameter
 419 value) remained consistent and (b) the MSE did not change significantly compared to the initial
 420 tests. (c) Using experimental data, the percentage of large parameter uncertainties decreased
 421 slightly and (d) the model predictions improved relative to the initial tests, but did not continue
 422 to improve as more data was added. Each round added 3 additional experiments, consisting of 5
 423 time points measured for each experiment. For the DoE rounds, 3 experiments chosen from the
 424 top 20 experiments suggested by the DoE algorithm were added. For the control rounds, data

425 from 3 initial conditions not included in the DoE suggestions were added (50 mM Gly, 25 mM
426 Gly and 25 mM Ala, and 50 mM Ala).

427 In our preliminary tests using simulated data with artificial noise, adding results from
428 experiments suggested by the DoE method did not reduce the number of parameters with large
429 standard deviations or improve the accuracy of the model predictions. This suggests that the poor
430 precision of the parameter estimates may not be caused by poor data coverage, and is instead a
431 consequence of the model structure. When applied to our experimental data, the addition of
432 results suggested by the algorithm did decrease the number of parameters with large standard
433 deviations and improved the model predictions relative to the initial tests, however, there was
434 significantly less improvement from the second round of additional experiments than there was
435 in the first. The simulated results suggest a limit to how much additional data can improve the
436 parameter estimates and highlight that the model structure is responsible for sloppiness. Even
437 after nearly doubling the amount of data included in our original tests, neither the experimental
438 nor the simulated system ever had fewer than 60% of parameters with large standard deviations
439 and the model predictions were essentially unchanged. Overall, it seems unlikely that continued
440 cycles would significantly improve the parameter estimates to the extent that it would allow us to
441 attach any physical significance to their numerical values.

442 Data suggested by the DoE algorithm typically had similar or better performance than the
443 data that was added arbitrarily. However, we cannot conclude there is a significant improvement
444 from using the DoE algorithm, because during the second round of experiments using arbitrary
445 data produced very similar results in all cases. Concerning the experimental results, conclusively
446 determining whether the selections of the DoE algorithm are an improvement over randomly
447 selected conditions would require performing many additional experiments. Within the existing
448 results, we noted that model prediction errors occasionally increased when more data was added,
449 which can be a consequence of overfitting, however, there was no consistent trend of samples
450 outside of the training data set having significantly higher prediction errors, suggesting
451 overfitting is not likely (Supplementary Information 6). Because the increases in prediction error
452 are small, they are probably an incidental consequence of the noise in the data and the limited
453 sample size.

454 There are several possible reasons why DoE did not consistently improve the precision
455 of the parameter estimates this model. The precision of a sloppy model is limited by the most
456 variable parts, so experimental noise may be preventing key features from being determined
457 more precisely (Gutenkunst et al. 2007a). The prescribed range of initial conditions may have
458 also been too restrictive. We only included initial conditions with various concentrations of
459 monomers because amino acids and peptides can participate in different reaction mechanisms
460 with TP. Since these mechanisms were not being explicitly separated in the model, initial
461 conditions with large concentrations of peptides could have inadvertently led to measuring the
462 parameters for a different reaction mechanism. Rather than risk measuring the kinetics of a
463 different mechanism, which would undermine the assumption that each experiment had the same

464 kinetic parameter value, we chose to use a more limited system definition. However, this also
465 may have limited our ability to constrain some parts of the network. Finally, as DoE methods are
466 statistically based approaches that rely on existing results, they can be sensitive to noise in the
467 data. As a result, it may be difficult to predict how parameter uncertainties will change as
468 additional data is added. Therefore, because sloppy networks tend to be better at producing
469 accurate predictions than accurate parameter estimates, approaches that aim to improve
470 predictions rather than parameter uncertainties may be more useful.

471 *Model Limitations*

472 The mass-action style model used here is a significant simplification of the reactions
473 occurring in the actual experimental system. TP-activated peptide bond formation involves not
474 only multiple intermediates but likely multiple reaction mechanisms, which were not fully
475 described in this model (Boigenzahn & Yin 2022). Certain products, like the cyclic dimers 2,5-
476 diketopiperazine were not detectable or quantifiable in our analysis. Merging the isomeric
477 peptide species also may have increased the experimental error slightly, since not all isomers
478 have the same absorbance. However, on average, the species balances of glycine and alanine
479 were about 90% accurate, suggesting that any products missed by our analysis were probably not
480 dominant products in the system. While we acknowledge the simplifications and sources of noise
481 in our experiments, it is important to note that the model generated high parameter standard
482 deviations when extremely small amounts of noise were added to simulated data. It may not be
483 possible to fit the current version of the peptide network with high precision from experimental
484 data.

485 It might be possible to alleviate sloppiness by replacing the generic reversible reactions in
486 this model with more detailed descriptions and measurements of intermediates. However, this
487 would significantly increase the resources needed for experimental and statistical analysis.
488 Additionally, this model does not account for increasing concentration of all species as the
489 sample dries. The volume could be included as a dynamic term in the network model, but it
490 complicates parameter estimation because of the infinite limits that occur as the volume
491 approaches zero. There are also potential reactions that occur almost exclusively in the solid
492 phase (Napier & Yin, 2006). We chose to neglect any concentration effects or details of the TP
493 reaction mechanism and instead explored the feasibility of creating a model that predicted
494 overall peptide production.

495 *Conclusion*

496 Although we were able to fit kinetic parameters to the peptide reaction network in our
497 simulated tests, in practice the parameter estimations were poorly constrained due to sloppiness.
498 Neither network reduction nor statistical design of experiments were particularly successful for
499 reducing sloppiness or improving the precision of the parameter estimates for this example.
500 Sloppiness precludes us from drawing any physical conclusions based on the individual values of
501 the parameters estimated in these models, but this approach is still an effective way to make

502 model predictions based on relatively few time points. The predictive capacity of the model may
 503 be useful for forming hypotheses about the behavior of systems that pass through multiple
 504 conditions sequentially, or simply estimating equilibrium conditions based on short-term
 505 experiments.

506 Our goal was not only to explore the kinetics of these specific reactions, but to evaluate the
 507 potential challenges and opportunities of applying mathematical tools, which were originally
 508 developed for biological networks to prebiotic chemical systems. Sloppiness is a challenge when
 509 studying the kinetics of complex nonlinear system models but may be an interesting property in
 510 the broader context of the chemical origins of life; sloppiness has been suggested as a possible
 511 non-adaptive explanation for the robustness of many multiparameter biological systems (Daniels
 512 et al. 2008). This idea suggests that many complex networks, ranging from those found in
 513 biology to those that are randomly generated, have similar behavior across large areas of the
 514 parameter space. This implies that robustness, in this case a reaction network's ability to achieve
 515 similar outcomes despite variation in its parameter values, can emerge from complexity even
 516 when it is not specifically selected for. The feature of intrinsic robustness in sufficiently large
 517 multiparameter networks observed in deep neural networks, which can be dramatically complex
 518 but highly accurate, and is an open area of investigation in the machine learning community
 519 (Belkin, et al. 2019). As a result, there is a significant incentive to work towards studying more
 520 complex experimental origins of life systems.

521 Adapting systems biology tools to study complex origins of life experiments lends itself to an
 522 interdisciplinary approach, since many methods can be difficult to implement or even approach
 523 without expert assistance. Demonstrative studies like this one can improve experimentalists'
 524 understanding of what data analysis approaches are available, what their limitations are, and
 525 what results they can provide. We hope that using computational networks to analyze
 526 experiments will become more commonplace and enable the study of more complex origins of
 527 life reaction networks.

528

529 *Computational Methods*

530 The usefulness of a parametric model is limited by our ability to accurately determine the
 531 values of the corresponding parameters. A large body of work has detailed various parameter
 532 fitting or regression techniques that can be used to build these models (Bard 1974). The most
 533 popular parameter estimation method is maximum likelihood estimation (MLE). In MLE, the
 534 noise from experimental measurements (ϵ) is treated as a random variable that captures the error
 535 between the model predictions and the observed output values:

$$536 \quad \mathbf{y} = m(\mathbf{X}; \boldsymbol{\theta}) + \boldsymbol{\epsilon} \quad (1)$$

537 Where $\boldsymbol{\epsilon} \in \mathbb{R}^S$, S is the number of observations (measurements) available, m is the model and
 538 $\boldsymbol{\theta} \in \mathbb{R}^n$ are its n parameters. The set of output observations is stored in the vector $\mathbf{y} \in \mathbb{R}^S$, and

539 $X \in \mathbb{R}^{S \times K}$, known as the design or feature matrix, is structured so that the s^{th} row corresponds to
 540 the s^{th} observation, \mathbf{x}_s , and the k^{th} column corresponds to the k^{th} input variable x_k . Combining
 541 MLE's assumption that $\boldsymbol{\theta}$ and X are deterministic variables with the most common noise model,
 542 the Gaussian or normal distribution ($(\epsilon \sim \mathcal{N}(0, \Sigma))$, where Σ is the covariance of the noise)
 543 allows us to exploit the fact that the sum of normal distributions is also a normal distribution. We
 544 can use this to calculate the distribution for the observations vector, $\mathbf{y} \sim \mathcal{N}(m(X, \boldsymbol{\theta}), \Sigma)$. The
 545 goal of MLE is then to find the values of $\boldsymbol{\theta}$ that best account for the experimental observations,
 546 or the values for $\boldsymbol{\theta}$ that best parameterize this output distribution. This is done by determining the
 547 values that maximize the log-likelihood function, $L(\boldsymbol{\theta})$:

$$548 \quad \boldsymbol{\theta}^* = \underset{\boldsymbol{\theta}}{\operatorname{argmax}} L(\boldsymbol{\theta}) = \underset{\boldsymbol{\theta}}{\operatorname{argmax}} \log f(\mathbf{y}|X, \boldsymbol{\theta}, \Sigma) \quad (2)$$

549 where $f(\mathbf{y}|X, \boldsymbol{\theta}, \Sigma)$ is the likelihood (or conditional probability) that the outputs in \mathbf{y} would be
 550 observed given values for X , $\boldsymbol{\theta}$, and Σ . For the given distribution of \mathbf{y} :

$$551 \quad f(\mathbf{y}|X, \boldsymbol{\theta}, \Sigma) = \left((2\pi)^{-\frac{S}{2}} |\Sigma|^{-\frac{1}{2}} \right) \exp \left(-\frac{1}{2} (\mathbf{y} - m(X; \boldsymbol{\theta}))^T \Sigma^{-1} (\mathbf{y} - m(X; \boldsymbol{\theta})) \right) \quad (3)$$

552 The well-known ordinary least squares regression problem is a special case of MLE where the
 553 model is linear and Σ is a diagonal matrix composed of identical values (σ^2).

554 A common issue with MLE is that (2) can have multiple solutions ($L(\boldsymbol{\theta})$ is nonconvex),
 555 as is often the case with nonlinear models. However, some of these solutions may contain
 556 parameter values that are not physically sensible, making the solution invalid. One way to
 557 overcome this limitation is to shift the goal of (2) from maximizing the probability of measuring
 558 the observed outputs given a set of parameters to maximizing the probability of a set of
 559 parameters being correct given a set of observations. Mathematically, this is done using Bayes'
 560 theorem, $f(\boldsymbol{\theta} | \mathbf{y}) \propto f(\mathbf{y} | \boldsymbol{\theta})f(\boldsymbol{\theta})$, and changes the likelihood function to:

$$561 \quad \boldsymbol{\theta}^* = \underset{\boldsymbol{\theta}}{\operatorname{argmax}} \log f(\mathbf{y}|X, \boldsymbol{\theta}, \Sigma) + \log f(\boldsymbol{\theta}) \quad (4)$$

562 where now we no longer assume that $\boldsymbol{\theta}$ is deterministic but instead has some distribution (e.g.,
 563 $\boldsymbol{\theta} \sim \mathcal{N}(\bar{\boldsymbol{\theta}}, \Sigma_{\boldsymbol{\theta}})$) that is captured by the prior $f(\boldsymbol{\theta})$. This term can be used to input any prior
 564 knowledge or expectation one might have over the values of the model parameters (e.g., must
 565 have a certain sign, lay within a specified range, etc.) and thereby constrain the search to values
 566 of $\boldsymbol{\theta}$ that satisfy the desired criteria. If \mathbf{y} and $\boldsymbol{\theta}$ are normally distributed, then (4) can be
 567 expressed as:

$$568 \quad \boldsymbol{\theta}^* = \underset{\boldsymbol{\theta}}{\operatorname{argmin}} \frac{1}{2} (\mathbf{y} - m(X; \boldsymbol{\theta}))^T \Sigma^{-1} (\mathbf{y} - m(X; \boldsymbol{\theta})) + \frac{1}{2} (\boldsymbol{\theta} - \bar{\boldsymbol{\theta}})^T \Sigma_{\boldsymbol{\theta}}^{-1} (\boldsymbol{\theta} - \bar{\boldsymbol{\theta}}) \quad (5)$$

569 Note that the first term will be minimized when the model predictions exactly match the output
 570 observations, while the second term will be minimized when $\boldsymbol{\theta} = \bar{\boldsymbol{\theta}}$. To perform the optimization

571 of model parameters, we use the L-BFGS-B algorithm from SciPy's minimize function with a
 572 tolerance for termination of 1e-3. As a result, Bayes' estimation seeks to balance the fit of the
 573 model with the prior knowledge over the parameters that is available. We use an Expectation-
 574 Maximization (EM) algorithm to determine the covariance matrix of the measurement noise and
 575 the parameter prior that maximizes the model evidence (Thompson et al. 2022).

576 Due to the randomness in \mathbf{y} , the selected parameters $\boldsymbol{\theta}^*$ will exhibit an inherent
 577 uncertainty that is determined by how well the estimates are constrained by experimental data.
 578 The parameter uncertainty is largely controlled by the model structure as well as the quality and
 579 quantity of the available data. If a model is selected where certain inputs are not strong predictors
 580 of the outputs or are dependent on other inputs, or if the dataset is too small or contains
 581 redundant samples, then $\boldsymbol{\theta}^*$ will be imprecise. This is a major issue as it can lead to overfitting,
 582 where m is not able to make accurate predictions at values of x that are outside of the dataset.

583 An estimate of the parameter uncertainty can be obtained from the eigenvalues of the
 584 Hessian matrix, $\mathcal{H}(\mathbf{y}; \boldsymbol{\theta})$, also known as the Fisher information matrix (FIM) in the context of
 585 parameter estimation, which is defined as:

$$586 \quad \mathcal{H}_{i,j} = \frac{\partial^2 L}{\partial \theta_i \partial \theta_j} \quad (6)$$

587 The eigenvalues of the Hessian serve as an estimate of data sufficiency. From calculus we know
 588 that the second derivative of a function, f'' , determines if a critical point ($f' = 0$) is a maximum
 589 ($f'' < 0$), a minimum ($f'' > 0$), or an inflection point ($f'' = 0$), which could be either a
 590 minimum, a maximum, or neither. Additionally, we can also estimate how sharp or defined an
 591 extremum is from the value of f'' . As a result, we can use $\mathcal{H}(\mathbf{y}; \boldsymbol{\theta})$ to gauge the quality of the
 592 obtained solution. For example, if all the eigenvalues of $\mathcal{H}(\mathbf{y}; \boldsymbol{\theta})$ are large and positive ($\gg 0$),
 593 this implies that $\boldsymbol{\theta}^*$ sits in a well-defined minimum and provides a precise estimate of the
 594 parameters. If all the eigenvalues are positive and one or more are small ($\ll 1$), then the
 595 minimum is not sharp, and the parameter estimates will be ill-defined and exhibit high
 596 variability. Finally, if $\mathcal{H}(\mathbf{y}; \boldsymbol{\theta})$ has any eigenvalues equal to zero, then $\boldsymbol{\theta}^*$ lays on a flat surface
 597 and cannot be uniquely estimated from the data; in other words, $\boldsymbol{\theta}^*$ has infinite variability.

598 If the precision of $\boldsymbol{\theta}^*$ is deemed to be too low, there are two methods that can be used to
 599 improve the quality of the estimates. The first, known as system identification, involves the
 600 structure of the model and the selection of the input variables. We can determine the relative
 601 importance of the input variables using a feature importance technique such as automatic
 602 relevance determination (ARD), or model class reliance (MCR), or as used in this paper, sparse
 603 principal component analysis (SPCA) (Zou et al. 2006). This information can then be used to
 604 restructure m to eliminate any redundant inputs.

605 If system identification is not able to reduce the uncertainty of the parameter estimates to
 606 a desired level, a second approach is to collect additional data. However, the data must provide

607 additional information beyond what is already contained in the current dataset to have any
 608 chance of improving the parameter estimates. One way to achieve this is by using a design of
 609 experiments (DoE) algorithm to select experiments that have a maximal value. Depending on the
 610 goal of the experiments (optimization, discovery, or both), their value can be measured by the
 611 information content they provide or by their predicted proximity to a desired set of properties.
 612 There is a rich variety of DoE algorithms to select from such as response surface methodology
 613 (RSM), screening, factorial design, etc. (Fisher 1937; Box & Wilson 1951; Shevlin 2017). A
 614 common metric to evaluate the optimality of candidate experimental designs is the determinant
 615 of the FIM. For any candidate experimental design, X , the FIM is computed as

$$616 \quad \mathcal{H}_{i,j} = \frac{\partial^2 L}{\partial \theta_i \partial \theta_j} = \Sigma_{\theta_{i,j}}^{-1} + \frac{\partial m(X, \boldsymbol{\theta})}{\partial \theta_i} \Sigma^{-1} \frac{\partial m(X, \boldsymbol{\theta})}{\partial \theta_j} \quad (7)$$

617 where evaluations of the gradient with respect to model parameters is computed using the
 618 forward sensitivity equations (Ma et al. 2021).

619 While DoE can be very useful for improving parameter uncertainties, there are several
 620 challenges. Calculating the expected information gain (EIG) can be time consuming due to the
 621 number of operations that need to be performed for larger systems. As a result, obtaining a new
 622 batch of experiments can easily take on the order of hours depending on the size of the dataset
 623 and the number of parameters involved. Even for moderately sized models, the quantity or
 624 precision of an experimental system may not be sufficient for accurate predictions of the
 625 information generated by each experiment to be made in the first place, or the experiments that
 626 would provide the information may not be feasible in reality. Both cases seriously hinder the
 627 effectiveness of DoE methods.

628 Selection of experiments for the DoE method was performed as in Thompson et al.
 629 (2022). Experimental data was normalized using linear scaling to ensure that the concentration
 630 values for each species spanned [0,1]. Scaling the data ensures that low abundance species still
 631 affect the parameter fits, which was necessary since the experimental results span several orders
 632 of magnitude. Parameters values were limited to [0,10] for simplicity, though we found that
 633 raising the upper bound had no effect if the initial guesses were single digit. Negative values had
 634 no physical meaning since both directions of the reversible reactions were already included. All
 635 computational methods were performed using Python 3.2.2. We used automatic differentiation in
 636 PyTorch to calculate the gradients of the loss function and SciPy to solve the initial value
 637 problems. Relevant code is available at <https://github.com/haboigenzahn/OoL-KineticParameterEstimation>.

639 Simulated data for testing was generated in Python 3.2.2 using SciPy 1.7.1 `solve_ivp`.
 640 The parameters for the simulated data were loosely based on the parameter fits of the
 641 experimental data, but were rounded to integers (Supplementary Information 7). Network figures
 642 were generated using Cytoscape 3.7.2 (Shannon et al. 1971).

643 *Experimental Materials & Methods*

644 All chemicals were of analytical grade purity and used without further purification.
645 Materials were obtained from suppliers as follows: trisodium trimetaphosphate (TP) and
646 trifluoroacetic acid (TFA) from Sigma-Aldrich, sodium hydroxide from Fisher Scientific, acetone
647 from Alfa Aesar, 9-fluorenylmethoxycarbonyl chloride (FMOC) from Creosalus, acetonitrile
648 from VWR Chemicals, and sodium tetraborate anhydrous from Acros Organics. Reactions were
649 carried out in 1.5 mL low-retention Eppendorf tubes. Peptide standards came from various
650 sources: glycine, diglycine, triglycine, pentaglycine, dialanine and Ala-Gly from Sigma-Aldrich,
651 tetraglycine from Bachem, Gly-Gly-Ala from Chem-Impex International, Ala-Gly-Gly from
652 ChemCruz, Ala-Ala-Gly from Pepmic, and Gly-Ala-Gly, Gly-Ala-Ala, Ala-Gly-Ala and
653 trialanine from Biomatik.

654 Samples were prepared with 0.15 M NaOH, various concentrations of glycine and
655 alanine, and TP in equimolar concentration to the total amount of amino acid. Details of the
656 initial conditions chosen are included in the supplemental information (Supplementary
657 Information 8). Samples were placed on a heat block preheated to 90°C with the caps open and
658 allowed to dry for 24 hours. At the end of each day of drying, samples were rehydrated with
659 1000 µL milliQ water preheated to about 65°C, capped and vortexed (Pulsing Vortex Mixer,
660 Fisher Scientific) 3000 rpm until everything was dissolved, which took 1-3 minutes per sample.

661 To analyze the samples with UV-HPLC, they were first derivatized using FMOC, which
662 increases the retention time and signal strength of peptide analytes. For the FMOC
663 derivatization, 25 µL of sample was diluted with 75 µL milliQ water to put the large monomer
664 peaks in a quantifiable range. Each sample was then mixed with 100 µL 0.1 M sodium
665 tetraborate buffer for pH control. Finally, 800 µL 3.125 mM FMOC dissolved in acetone was
666 added to each sample. For a sample of 0.1 M amino acid, this results in an equal concentration of
667 FMOC and amino acid, and a slight excess of FMOC in any samples where peptide bond
668 formation had occurred. Linear calibration curves were determined for all species using this
669 approach (Supplementary Information 9), which were used to estimate peptide concentration
670 based on the integrated absorbance values of the HPLC peaks of the samples.

671 Samples were analyzed with a Shimadzu Nexera HPLC with a C-18 column
672 (Phenomenex Aeris XB-C18, 150 mm x 4.6 mm, 3.6 µL). Products were measured at 254 nm.
673 UV-HPLC analysis was performed using Solvent A: milliQ water with 0.01% v/v trifluoroacetic
674 acid (TFA) and Solvent B: acetonitrile with 0.01% v/v TFA. The following gradient was used:
675 0-4 min, 30% B, 4-12 min, 30-100% B, 14-15 min, 100-30% B, 15-17 min, 30% B. The solvent
676 flow rate was 1 mL/min. Peak integration was performed using LabSolutions with the 'Drift'
677 parameter set to 10000.

678

679 **Declarations**

680 **Ethics Approval** No approvals required.

681 **Conflict of Interest** The authors declare no conflict of interest. The funders had no role in the design of
682 the study; in the collection, analyses, or interpretation of data; in the writing of the manuscript, or in the
683 decision to publish the results.

684 **Data Availability** The data shown in this study is available from John Yin upon reasonable request.

685 **Authors' Contributions** All experimental data was collected and analyzed by HB. The main parameter
686 estimation code was developed by JCT, with minor edits and applications performed by HB and LDG.
687 The manuscript was drafted by HB and LDG and all authors contributed to subsequent editing.

688 **Funding** This research was funded by the Vilas Distinguished Achievement Professorship, the Office
689 of the Vice Chancellor for Research and Graduate Education, the Wisconsin Institute for Discovery, all at
690 the University of Wisconsin-Madison; and the Wisconsin Alumni Research Foundation (WARF); grant
691 R01DK133605 from the National Institutes of Health; and grants MCB-2029281, CBET-2030750, and
692 DMS-2151959 from the US National Science Foundation. We also acknowledge support from the GERS
693 program at the University of Wisconsin-Madison.

694 **Consent to Publish** All authors read and approved the final manuscript.

695 **Acknowledgements** Thank you to Izabela Sibilska-Kaminski, who contributed to the experimental
696 background for this project, and to other members of the Yin lab as well as Prof. David Baum for their
697 thoughtful feedback. We further acknowledge financial support via the NSF-EFRI award 2132036 and the
698 Advanced Opportunity Fellowship from the University of Wisconsin-Madison Graduate Engineering
699 Research Scholars program.

700

701

702

703

704

705

706

707

708

709

710

711

712

713

714
715
716
717

718 **References**

719 Apgar, J. F., Witmer, D. K., White, F. M., & Tidor, B. (2010). Sloppy models, parameter uncertainty, and
720 the role of experimental design. *Molecular BioSystems*, 6(10), 1890–1900.
721 <https://doi.org/10.1039/b918098b>

722 Apri, M., de Gee, M., & Molenaar, J. (2012). Complexity reduction preserving dynamical behavior of
723 biochemical networks. *Journal of Theoretical Biology*, 304, 16–26.
724 <https://doi.org/10.1016/j.jtbi.2012.03.019>

725 Bard, Y. (1974). *Nonlinear parameter estimation* (No. 04; QA276. 8, B3.).

726 Belkin, M., Hsu, D., Ma, S., & Mandal, S. (2019). Reconciling modern machine-learning practice and the
727 classical bias–variance trade-off. *Proceedings of the National Academy of Sciences*, 116(32), 15849–
728 15854. <https://doi.org/10.1073/pnas.1903070116>

729 Box, G. E. P. and Wilson K. B. (1951) On the experimental attainment of optimum conditions. *Journal of
730 the Royal Statistical Society*, 13, 1-45. <https://doi.org/10.1111/j.2517-6161.1951.tb00067.x>

731 Brown, K. S., Hill, C. C., Calero, G. A., Myers, C. R., Lee, K. H., Sethna, J. P., & Cerione, R. A. (2004).
732 The statistical mechanics of complex signaling networks: Nerve growth factor signaling. *Physical
733 Biology*, 1(3), 184–195. <https://doi.org/10.1088/1478-3967/1/3/006>

734 Brown, K. S., & Sethna, J. P. (2003). Statistical mechanical approaches to models with many poorly
735 known parameters. *Physical Review E - Statistical Physics, Plasmas, Fluids, and Related
736 Interdisciplinary Topics*, 68(2), 9. <https://doi.org/10.1103/PhysRevE.68.021904>

737 Chaloner, K., & Verdinelli, I. (1995). Bayesian Experimental Design: A Review. *Statistical Science*,
738 10(3), 273–304.

739 Chis, O.-T., Banga, J. R., & Balsa-Canto, E. (2014). *Sloppy models can be identifiable*. 1–35.
740 <http://arxiv.org/abs/1403.1417>

741 Cobelli, C., & DiStefano, J. J. (1980). Parameter and structural identifiability concepts and ambiguities: a
742 critical review and analysis. *The American Journal of Physiology*, 239(1), 7–24.
743 <https://doi.org/10.1152/ajpregu.1980.239.1.R7>

744 Coveney, P. V., Swadling, J. B., Wattis, J. A. D., & Greenwell, H. C. (2012). Theory, modelling and
745 simulation in origins of life studies. *Chemical Society Reviews*, 41(16), 5430–5446.
746 <https://doi.org/10.1039/c2cs35018a>

747 Daniels, B. C., Chen, Y. J., Sethna, J. P., Gutenkunst, R. N., & Myers, C. R. (2008). Sloppiness,
748 robustness, and evolvability in systems biology. *Current Opinion in Biotechnology*, 19(4), 389–395.
749 <https://doi.org/10.1016/j.copbio.2008.06.008>

750 Fisher, R. A. (1937). *Design of experiments*. Edinburgh: Oliver and Boyd, 1935.

751 Frenkel-Pinter, M., Samanta, M., Ashkenasy, G., & Leman, L. J. (2020). Prebiotic Peptides: Molecular
752 Hubs in the Origin of Life. *Chemical Reviews*, 120(11), 4707–4765.
753 <https://doi.org/10.1021/acs.chemrev.9b00664>

754 Gauthier, J., Vincent, A. T., Charette, S. J., & Derome, N. (2019). A brief history of bioinformatics.
755 *Briefings in Bioinformatics*, 20(6), 1981–1996. <https://doi.org/10.1093/bib/bby063>

756 Goldman, A. D., Bernhard, T. M., Dolzhenko, E., & Landweber, L. F. (2013). LUCApedia: A database
757 for the study of ancient life. *Nucleic Acids Research*, 41(D1), 1079–1082.
758 <https://doi.org/10.1093/nar/gks1217>

759 Gutenkunst, R. N., Casey, F. P., Waterfall, J. J., Myers, C. R., & Sethna, J. P. (2007). Extracting
760 falsifiable predictions from sloppy models. *Annals of the New York Academy of Sciences*, 1115,
761 203–211. <https://doi.org/10.1196/annals.1407.003>

762 Gutenkunst, R. N., Waterfall, J. J., Casey, F. P., Brown, K. S., Myers, C. R., & Sethna, J. P. (2007a).
763 Universally sloppy parameter sensitivities in systems biology models. *PLoS Computational Biology*,
764 3(10), 1871–1878. <https://doi.org/10.1371/journal.pcbi.0030189>

765 Hettling, H., & van Beek, J. H. G. M. (2011). Analyzing the functional properties of the creatine kinase
766 system with multiscale “sloppy” modeling. *PLoS Computational Biology*, 7(8), 11–16.
767 <https://doi.org/10.1371/journal.pcbi.1002130>

768 Lee, D. H., Granja, J. R., Martinez, J. A., Severin, K., & Ghadiri, M. R. (1996). A self-replicating peptide.
769 *Nature*, 382, 525–528.

770 Ludlow, R. F., & Otto, S. (2008). Systems chemistry. *Chemical Society Reviews*, 37(1), 101–108.
771 <https://doi.org/10.1039/b611921m>

772 Jagadeesan, P., Raman, K., & Tangirala, A. K. (2022). Bayesian Optimal Experiment Design for Sloppy
773 Systems. *IFAC-PapersOnLine*, 55(23), 121-126. <https://doi.org/10.1016/j.ifacol.2023.01.026>

774 Jain, A., McPhee, S. A., Wang, T., Nair, M. N., Kroiss, D., Jia, T. Z., & Ulijn, R. V. (2022). Tractable
775 molecular adaptation patterns in a designed complex peptide system. *Chem*, 8(7), 1894–1905.
776 <https://doi.org/10.1016/j.chempr.2022.03.016>

777 Johnson, E. O., & Hung, D. T. (2019). A Point of Inflection and Reflection on Systems Chemical
778 Biology. *ACS Chemical Biology*, 14(12), 2497–2511. <https://doi.org/10.1021/acschembio.9b00714>

779 Ma, S., & Dai, Y. (2011). Principal component analysis based methods in bioinformatics studies.
780 *Briefings in Bioinformatics*, 12(6), 714–722. <https://doi.org/10.1093/bib/bbq090>

781 Ma, Y., Dixit, V., Innes, M. J., Guo, X., & Rackauckas, C. (2021). A Comparison of Automatic
 782 Differentiation and Continuous Sensitivity Analysis for Derivatives of Differential Equation
 783 Solutions. *2021 IEEE High Performance Extreme Computing Conference, HPEC 2021*, 2,
 784 1–9. <https://doi.org/10.1109/HPEC49654.2021.9622796>

785 Maity, S., Ottelé, J., Santiago, G. M., Frederix, P. W. J. M., Kroon, P., Markovitch, O., ... Roos,
 786 W. H. (2020). Caught in the Act: Mechanistic Insight into Supramolecular Polymerization-
 787 Driven Self-Replication from Real-Time Visualization. *Journal of the American Chemical
 788 Society*, 142(32), 13709–13717. <https://doi.org/10.1021/jacs.0c02635>

789 Maiwald, T., Hass, H., Steiert, B., Vanlier, J., Engesser, R., Raue, A., Kipkeew, F., Bock, H. H., Kaschek,
 790 D., Kreutz, C., & Timmer, J. (2016). Driving the model to its limit: Profile likelihood based model
 791 reduction. *PLoS ONE*, 11(9), 1–18. <https://doi.org/10.1371/journal.pone.0162366>

792 Mamajanov, I., Macdonald, P. J., Ying, J., Duncanson, D. M., Dowdy, G. R., Walker, C. A., Engelhart,
 793 A. E., Fernández, F. M., Grover, M. A., Hud, N. V., & Schork, F. J. (2014). Ester formation and
 794 hydrolysis during wet-dry cycles: Generation of far-from-equilibrium polymers in a model prebiotic
 795 reaction. *Macromolecules*, 47(4), 1334–1343. <https://doi.org/10.1021/ma402256d>

796 Maria, G. (2004). A review of algorithms and trends in kinetic model identification for chemical and
 797 biochemical systems. *Chemical and Biochemical Engineering Quarterly*, 18(3), 195–222.

798 Monsalve-Bravo, G. M., Lawson, B. A. J., Drovandi, C., Burrage, K., Brown, K. S., Baker, C. M.,
 799 Vollert, S. A., Mengersen, K., McDonald-Madden, E., & Adams, M. P. (2022). Analysis of
 800 sloppiness in model simulations: Unveiling parameter uncertainty when mathematical models are
 801 fitted to data. *Science Advances*, 8(38). <https://doi.org/10.1126/sciadv.abm5952>

802 Napier, J., & Yin, J. (2006). Formation of peptides in the dry state. *Peptides*, 27(4), 607–610.
 803 <https://doi.org/10.1016/j.peptides.2005.07.015>

804 Newman, M. E. (2003). The structure and function of complex networks. *SIAM review*, 45(2), 167–256.
 805 <https://doi.org/10.1137/S003614450342480>

806 Nghe, P., Hordijk, W., Kauffman, S. A., Walker, S. I., Schmidt, F. J., Kemble, H., Yeates, J. A. M., &
 807 Lehman, N. (2015). Prebiotic network evolution: Six key parameters. *Molecular BioSystems*,
 808 11(12), 3206–3217. <https://doi.org/10.1039/c5mb00593k>

809 Orgel, L. E. (2010). The origin of life: A review of facts and speculation. *The Nature of Life: Classical
 810 and Contemporary Perspectives from Philosophy and Science*, 0004(December), 121–128.
 811 <https://doi.org/10.1017/CBO9780511730191.012>

812 Raue, A., Schilling, M., Bachmann, J., Matteson, A., Schelke, M., Kaschek, D., Hug, S., Kreutz, C.,
 813 Harms, B. D., Theis, F. J., Klingmüller, U., & Timmer, J. (2013). Lessons Learned from
 814 Quantitative Dynamical Modeling in Systems Biology. *PLoS ONE*, 8(9).
 815 <https://doi.org/10.1371/journal.pone.0074335>

816 Rodriguez-Fernandez, M., Mendes, P., & Banga, J. R. (2006). A hybrid approach for efficient and robust
 817 parameter estimation in biochemical pathways. *BioSystems*, 83(2-3 SPEC. ISS.), 248–265.
 818 <https://doi.org/10.1016/j.biosystems.2005.06.016>

819 Rout, S. K., Rhyner, D., Riek, R., & Greenwald, J. (2022). Prebiotically Plausible Autocatalytic Peptide
820 Amyloids. *Chemistry - A European Journal*, 28(3). <https://doi.org/10.1002/chem.202103841>

821 Ruder, S. (2016). An overview of gradient descent optimization algorithms. *arXiv Preprint*
822 *arXiv:1609.04747*. <http://arxiv.org/abs/1609.04747>

823 Ruiz-Mirazo, K., Briones, C., & De La Escosura, A. (2014). Prebiotic systems chemistry: New
824 perspectives for the origins of life. *Chemical Reviews*, 114(1), 285–366.
825 <https://doi.org/10.1021/cr2004844>

826 Sakata, K., Kitadai, N., & Yokoyama, T. (2010). Effects of pH and temperature on dimerization rate of
827 glycine: Evaluation of favorable environmental conditions for chemical evolution of life.
828 *Geochimica et Cosmochimica Acta*, 74(23), 6841–6851. <https://doi.org/10.1016/j.gca.2010.08.032>

829 Schwartz, A. W. (2007). Intractable mixtures and the origin of life. *Chemistry and Biodiversity*, 4(4),
830 656–664. <https://doi.org/10.1002/cbdv.200790056>

831 Serov, N. Y., Shtyrlin, V. G., & Khayarov, K. R. (2020). The kinetics and mechanisms of reactions in the
832 flow systems glycine–sodium trimetaphosphate–imidazoles: the crucial role of imidazoles in
833 prebiotic peptide syntheses. *Amino Acids*, 52(5), 811–821. <https://doi.org/10.1007/s00726-020-02854-z>

835 Shannon, P., Markiel, A., Ozier, O., Baliga, N. S., Wang, J. T., Ramage, D., Amin, N., Schwikowski, B.,
836 & Ideker, T. (1971). Cytoscape: A Software Environment for Integrated Models. *Genome Research*,
837 13(22), 426. <https://doi.org/10.1101/gr.1239303.metabolite>

838 Shevlin, M. (2017). Practical high-throughput experimentation for chemists. *ACS medicinal chemistry
839 letters*, 8(6), 601–607. <https://doi.org/10.1021/acsmedchemlett.7b00165>

840 Sibilska, I., Feng, Y., Li, L., & Yin, J. (2018). Trimetaphosphate Activates Prebiotic Peptide Synthesis
841 across a Wide Range of Temperature and pH. *Origins of Life and Evolution of Biospheres*, 48(3),
842 277–287. <https://doi.org/10.1007/s11084-018-9564-7>

843 Surman, A. J., Rodriguez-Garcia, M., Abul-Haija, Y. M., Cooper, G. J. T., Gromski, P. S., Turk-
844 MacLeod, R., Mullin, M., Mathis, C., Walker, S. I., & Cronin, L. (2019). Environmental control
845 programs the emergence of distinct functional ensembles from unconstrained chemical reactions.
846 *Proceedings of the National Academy of Sciences*, 116(12), 5387–5392.
847 <https://doi.org/10.1073/pnas.1813987116>

848 Thompson, J. C., Zavala, V. M., & Venturelli, O. S. (2022). Integrating a tailored recurrent neural
849 network with Bayesian experimental design to optimize microbial community functions. *BioRxiv*, 1–
850 24.

851 Transtrum, M. K., Machta, B. B., Brown, K. S., Daniels, B. C., Myers, C. R., & Sethna, J. P. (2015).
852 Perspective: Sloppiness and emergent theories in physics, biology, and beyond. *Journal of Chemical
853 Physics*, 143(1). <https://doi.org/10.1063/1.4923066>

854 Transtrum, M. K., & Qiu, P. (2012). Optimal experiment selection for parameter estimation in biological
855 differential equation models. *BMC bioinformatics*, 13(1), 1-12. <https://doi.org/10.1186/1471-2105-13-181>

857 Vanlier, J., Tiemann, C. A., Hilbers, P. A. J., & van Riel, N. A. W. (2013). Parameter uncertainty
858 in biochemical models described by ordinary differential equations. *Mathematical
859 Biosciences*, 246(2), 305–314. <https://doi.org/10.1016/j.mbs.2013.03.006>

860 Varfolomeev, S. D., & Lushchekina, S. V. (2014). Prebiotic synthesis and selection of macromolecules:
861 Thermal cycling as a condition for synthesis and combinatorial selection. *Geochemistry
862 International*, 52(13), 1197–1206. <https://doi.org/10.1134/S0016702914130102>

863 Virtanen, P., Gommers, R., Oliphant, T. E., Haberland, M., Reddy, T., Cournapeau, D.,
864 Burovski, E., Peterson, P., Weckesser, W., Bright, J., van der Walt, S. J., Brett, M., Wilson,
865 J., Millman, K. J., Mayorov, N., Nelson, A. R. J., Jones, E., Kern, R., Larson, E., ...
866 Vázquez-Baeza, Y. (2020). SciPy 1.0: fundamental algorithms for scientific computing in
867 Python. *Nature Methods*, 17(3), 261–272. <https://doi.org/10.1038/s41592-019-0686-2>

868 von Kiedrowski, G. (1986). A Self-Replicating Hexdeoxynucleotide. *Angewandte Chemie - International
869 Edition*, 25(10), 932–935. <https://doi.org/10.1002/anie.198609322>

870 Wasserman, L. (2004). *All of statistics: a concise course in statistical inference* (Vol. 26, p. 86). New
871 York: Springer.

872 Waterfall, J. J., Casey, F. P., Gutenkunst, R. N., Brown, K. S., Myers, C. R., Brouwer, P. W., Elser, V., &
873 Sethna, J. P. (2006). Sloppy-model universality class and the vandermonde matrix. *Physical Review
874 Letters*, 97(15), 1–4. <https://doi.org/10.1103/PhysRevLett.97.150601>

875 White, A., Tolman, M., Thames, H. D., Withers, H. R., Mason, K. A., & Transtrum, M. K. (2016). The
876 Limitations of Model-Based Experimental Design and Parameter Estimation in Sloppy Systems.
877 *PLoS Computational Biology*, 12(12), 1–26. <https://doi.org/10.1371/journal.pcbi.1005227>

878 Wieland, F. G., Hauber, A. L., Rosenblatt, M., Tönsing, C., & Timmer, J. (2021). On structural and
879 practical identifiability. *Current Opinion in Systems Biology*, 25, 60–69.
880 <https://doi.org/10.1016/j.coisb.2021.03.005>

881 Yu, S. S., Krishnamurthy, R., Fernández, F. M., Hud, N. V., Schork, F. J., & Grover, M. A. (2016).
882 Kinetics of prebiotic depsipeptide formation from the ester-amide exchange reaction. *Physical
883 Chemistry Chemical Physics*, 18(41), 28441–28450. <https://doi.org/10.1039/c6cp05527c>

884 Zou, H., Hastie, T., & Tibshirani, R. (2006). Sparse principal component analysis. *Journal of
885 Computational and Graphical Statistics*, 15(2), 265–286.
886 <https://doi.org/10.1198/106186006X113430>